ELSEVIER

Polymer 41 (2000) 8041–8052

polymer

www.elsevier.nl/locate/polymer

Reactive compatibilization of nylon 6/styrene–acrylonitrile copolymer blends. Part 1. Phase inversion behavior

N. Kitayama[1], H. Keskkula, D.R. Paul*

Department of Chemical Engineering and Center for Polymer Research, The University of Texas at Austin, Austin, TX 78712, USA

Received 12 November 1999; received in revised form 16 February 2000; accepted 18 February 2000

Abstract

The phase morphology and phase inversion behavior of nylon 6 (PA)/styrene–acrylonitrile (SAN) compatibilized blends have been studied using an imidized acrylic polymer (IA) and a styrene/acrylonitrile/maleic anhydride terpolymer (SANMA) as compatibilizers. PA/SAN blends can be considered as a simpler version of industrially important PA/ABS blends; therefore, this study is useful for the better understanding of the morphology development for PA/ABS blends with compatibilizers. Compared to binary blends of nylon 6 and SAN, addition of IA causes the phase inversion composition to shift to a higher nylon 6 volume fraction; whereas, addition of SANMA slightly changes the phase inversion composition to a lower nylon 6 volume fraction. The use of IA results in a significant increase of the nylon 6 phase viscosity due to the in situ formation of graft polymers during the melt processing; whereas, the addition of SANMA only slightly increases the nylon 6 phase viscosity. The significant change in the nylon 6 to SAN25 viscosity ratio due to the formation of PA–IA graft polymer may be partially responsible for the shift of the phase inversion composition observed as addition of IA. The method of the mixing also affects the phase inversion composition. The composition range where the nylon 6 forms a continuous phase extends to a lower nylon 6 volume fraction for blends mixed in an extruder compared to those prepared in a Brabender. The stabilization of blend morphology by formation of graft copolymers was studied for compositions near phase inversion as well as at compositions away from this region. Accordingly, it has been shown that IA does not stabilize the morphology near the phase inversion composition, but it is very effective at compositions where either of the components forms a clearly defined dispersed phase. The factors affecting the critical composition where phase inversion occurs have been established.

Keywords: Nylon 6; Styrene/acrylonitrile; Imidized acrylic polymer

1. Introduction

Many new products have been manufactured by melt blending of polymers to achieve improved properties generally not available in any single polymeric material, e.g. toughness, chemical resistance, ease of fabrication, etc. [1]. The development of entirely new chemical structures is costly and time consuming in comparison to a simple melt blending approach. The in situ formation of graft or block copolymers to serve as compatibilizers during melt processing via the use of the appropriate reactive functionalities, i.e. reactive compatibilization [2], has emerged as an effective way of solving the problem associated with incompatible polymer mixtures. Reactive compatibilization of polyamide (PA) based blends generally makes use of the high reactivity of the polyamide amine end groups with anhydride functionality that can be incorporated in the second phase [3–32]. The work described here was motivated by the current industrial interest in compatibilized blends of polyamides with ABS materials [33–39].

Majumdar et al. [16,40] studied the mechanical properties and morphology of PA/ABS blends compatibilized with imidized acrylic polymers (IA) which are miscible with the styrene–acrylonitrile copolymer (SAN) matrix of ABS and has glutaric anhydride and methacrylic acid functionalities which can react with the amine end groups of polyamides. Majumdar et al. [15,41] examined the compatibilization of PA/SAN blends with a series of imidized acrylic polymers having varied functionality for reaction and miscibility with SAN. Styrene–acrylonitrile–maleic anhydride terpolymers (SANMA) may also be miscible with SAN, and the maleic anhydride portion reacts with amine end group of polyamide [33,34,38,42].

The purpose of this study is to explore the phase

---

* Corresponding author. Tel.: + 1-512-471-5238; fax: + 1-512-471-7060.

E-mail address: drp@che.utexas.edu (D.R. Paul).

[1] Permanent address: Mitsubishi Gas Chemical Co. Inc., Mitsubishi Bldg., 5-2, Marunouchi 2-chome, Chiyoda-ku, Tokyo, 100-0005, Japan.

0032-3861/00/$ - see front matter © 2000 Elsevier Science Ltd. All rights reserved.
PII: S0032-3861(00)00156-7

Table 1
Materials use in this study

Designation used here	Supplier Designation	Composition	Molecular weight [g/mol]	Brabender Torque [N m][a]	Source
L-PA (nylon 6)	Capron 8202	End-group content $NH_2 = 59.1\ \mu eq/g$ $COOH = 60.8\ \mu eq/g$	$\bar{M}_n = 16,700$	3.0	Allied Signal
M-PA (nylon 6)	Capron 8207F	End-group content $NH_2 = 47.9\ \mu eq/g$ $COOH = 43.0\ \mu eq/g$	$\bar{M}_n = 22,000$	6.0	Allied Signal
H-PA (nylon 6)	Capron 8209F	End-group content $NH_2 = 34.8\ \mu eq/g$ $COOH = 28.8\ \mu eq/g$	$\bar{M}_n = 29,300$	11.5	Allied Signal
SAN25 (styrene/acrylonitrile)	Tyril 100	25 wt% AN	$\bar{M}_w = 152,000$	6.6	Dow Chemical
SAN32.5 (styrene/acrylonitrile)	Lustran	32.5 wt% AN	$\bar{M}_w = 130,000$ $\bar{M}_n = 59,000$	6.0	Bayer
IA	EXL4140	55.7% methyl glutarimide 56.0% methyl methacrylate 2.18% methacrylic acid 1.08 % glutaric anhydride	$\bar{M}_w = 95,000$	–	Rohm & Haas
SANMA	–	65.7% styrene 33.0% acrylonitrile 1.3% maleic anhydride	$\bar{M}_n = 56,600$ $\bar{M}_w = 119,400$	–	Bayer

[a] Values taken at 240°C and 60 rpm after 10 min.

morphology and phase inversion behavior of nylon 6/SAN blends. The two-phase nature of ABS materials plus their high melt viscosity/elasticity complicates the morphological study of PA/ABS blends. Thus, PA/SAN blends are useful for the better understanding of the morphology development with compatibilizers. It is of particular interest to establish the range of co-continuous morphologies and the limiting phase ratios where one of the components is dispersed as discrete particles, since the mechanical properties depend on which component forms the continuous phase. Some commercial PA/ABS blends appear to have a co-continuous morphology [33,34,38]. However, relatively few studies [43,44] cover the complete range of compositions, i.e. from compositions where the SAN phase is continuous, through the phase inversion range to regions where the polyamide phase is continuous.

This paper compares the effects of two different compatibilizers, i.e. IA and SANMA, on the phase inversion characteristics of nylon 6/SAN blends. The type of mixing device used for melt blending, as shown here, can have an important effect on phase inversion behavior. The factors affecting the critical composition where phase inversion occurs have been established.

2. Experimental

Table 1 summarizes pertinent information about the materials used in this series of papers including three commercially available nylon 6 materials with different molecular weights labeled L for low, M for medium, and H for high. Two SAN materials with different AN contents were used; however, only SAN25 with an acrylonitrile (AN) content typical of many commercial ABS materials was used in this paper. Fig. 1 shows the chemical structures of the two compatibilizers used: the imidized acrylic polymer (IA) and the styrene/acrylonitrile/maleic anhydride terpolymer (SANMA). More detailed descriptions of these compatibilizers and the potential reactions they undergo are provided elsewhere [15,42].

A Brabender Plasticorder outfitted with a 50 ml mixing head and standard rotors was employed for melt rheological characterization and the preparation of some samples. Sixty grams of pre-mixed polymer pellets were added to the Brabender mixing chamber, preheated to 240°C, and mixed at 60 rpm. The blend compositions described in this series of papers were all prepared on a weight basis but some graphs, however, use polyamide volume fraction. In these cases, the volumes of the components were calculated from the following densities: polyamide $= 1.13\ g/cm^3$, SAN $= 1.07\ g/cm^3$, IA $= 1.18\ g/cm^3$.

The average particle size becomes constant in less than 10 min of mixing in the Brabender [45]. Therefore, small samples were taken from the Brabender chamber with metal spatulas at 10 min of mixing for TEM analysis; care was taken not to elongate or orient the sample in order to avoid altering the blend morphology. The samples were immediately quenched into liquid nitrogen.

Samples were also prepared by simultaneous extrusion of all components in a Killion single-screw extruder ($L/D = 30$, $D = 25.4$ mm) at 240°C using a screw speed of 40 rpm.

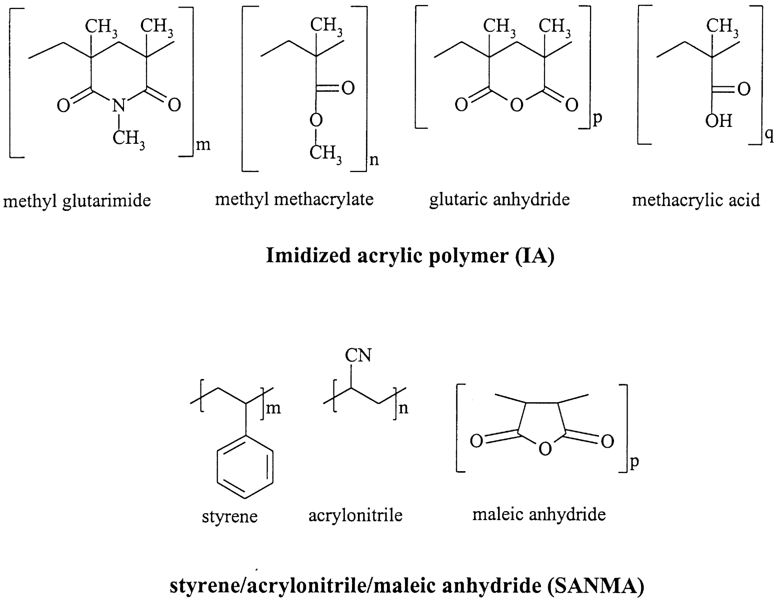

Fig. 1. Main repeat units of the imidized acrylic polymer (IA) and the styrene/acrylonitrile/maleic anhydride terpolymer (SANMA) used as compatibilizers.

The extrudate was drawn through a water bath and pelletized. All materials were dried in a vacuum oven at 80°C for at least one day prior to all melt-mixing operations.

Transmission electron microscopy (TEM) was used to observe the blend morphology. Specimens were cryogenically microtomed at −40°C from the center of extruded pellets into thin sections using a Reichert–Jung Ultracut E microtome outfitted with a diamond knife, parallel to the Brabender sample surface or perpendicular to the flow direction. The nylon 6 phase of the blends was preferentially stained by floating the sections on the surface of a 2% solution of phosphotungstic acid in order to generate sharp contrast between nylon 6 and SAN. TEM imaging was carried out on a Jeol 200CX microscope operating at an accelerating voltage of 120 keV.

A semi-automatic digital image analysis technique (NIH Image software®) was employed to determine the effective number average, $\bar{d}_n$, and weight average, $\bar{d}_w$, particle diameters from TEM photomicrographs. No corrections were applied to adjust for the fact that the sections are not cut from the equators of the particles; however, for the accurate statistical samplings, more than 200 particles from multiple TEM photomicrographs were analyzed.

3. Results and discussion

3.1. Shift of the phase inversion composition

Bourry et al. [46], Hietaoja et al. [7], and Zhang et al. [32] reported that addition of a compatibilizer does not affect the composition where phase inversion occurs. Dedecker et al. [6], however, reported that the composition range where co-continuity occurs for PA/PMMA blends was shifted to a lower polyamide content when a styrene–maleic anhydride copolymer was added as a compatibilizer.

For the blends prepared here in the Brabender, the phase inversion composition shifts to a higher polyamide volume fraction upon addition of IA. This trend is observed for all three nylon 6 materials regardless of their molecular weight. The results for M-PA/SAN25 blends shown in Fig. 2 is representative. The dotted line represents the phase inversion region. The filled circles, open circles, and shaded circles represent nylon 6 continuous, SAN continuous and co-continuous phase morphology, respectively.

Without any compatibilizer, phase inversion occurs at a nylon 6 volume fraction of about 0.48. By the addition of IA, the phase inversion composition shifts to a higher

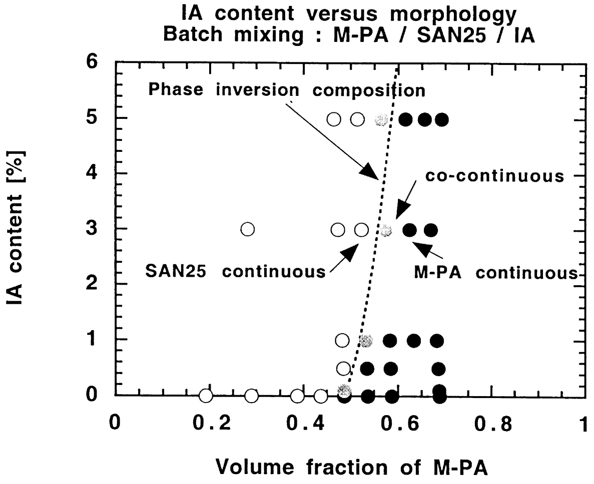

Fig. 2. Effect of IA content on the phase inversion composition of M-PA/SAN25 blends prepared in a Brabender batch mixer.

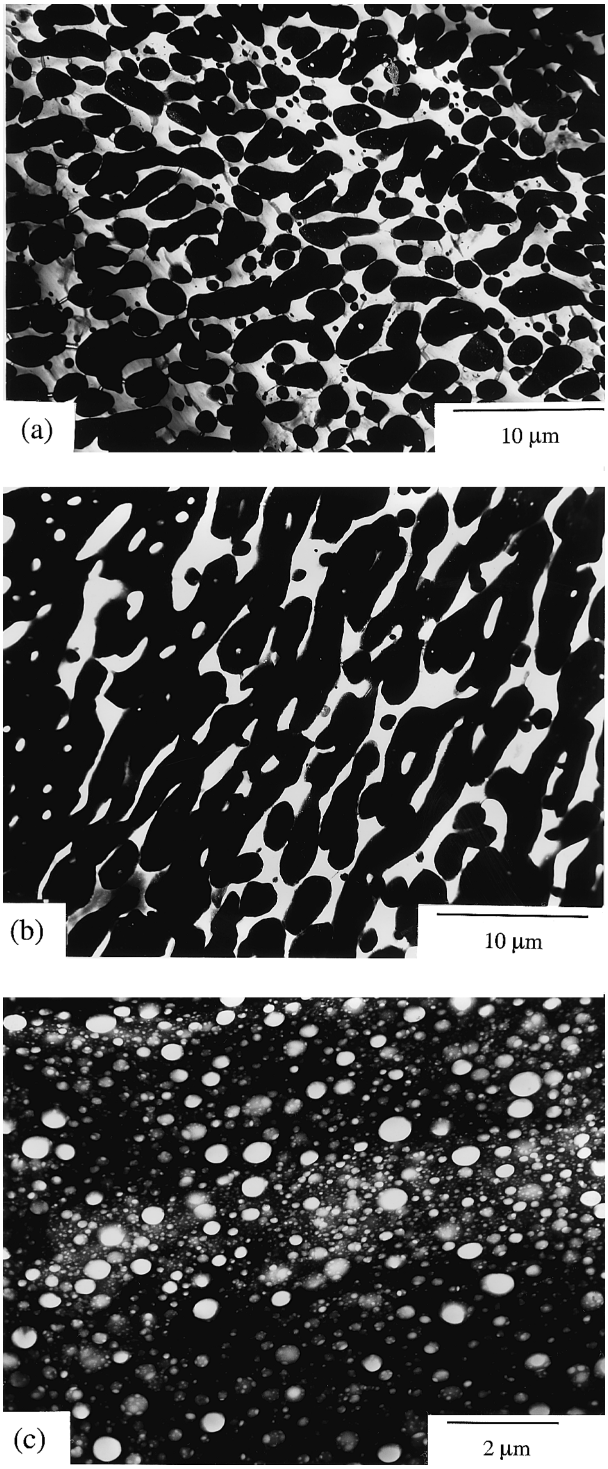

Fig. 3. TEM photomicrographs of ternary M-PA/SAN25/IA blends: (a) 53.5/43.5/3; (b) 58.5/38.5/3; (c) 67.9/29.1/3. The nylon 6 phase has been stained dark with phosphotungstic acid (PTA).

nylon 6 volume fraction. Co-continuous morphologies are observed for blends with transitional compositions (±5%).

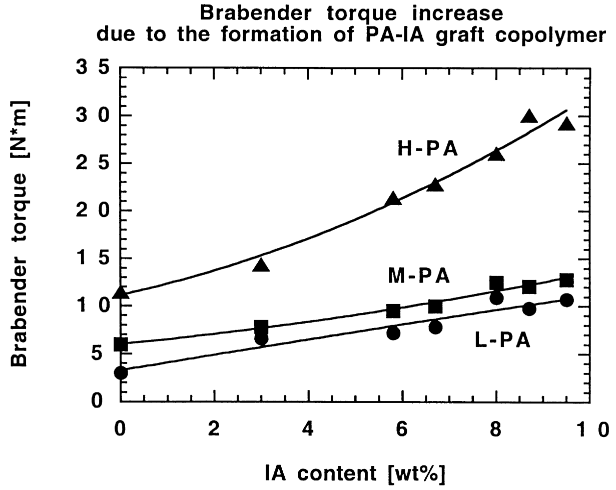

Fig. 4. Brabender torque increase due to the formation of PA–IA graft copolymer.

The TEM photomicrographs in Fig. 3 illustrate the transition from SAN25 being the continuous phase to an M-PA continuous phase as the nylon 6 volume fraction increases. When SAN25 is the continuous phase, the dispersed M-PA domains are fairly large and irregularly shaped. However, when M-PA is the continuous phase, SAN25 forms small and spherical domains. The effect of addition of compatibilizer on the size of the dispersed particles will be discussed more fully in Part 2 of this series.

3.2. *Effect of grafting reaction on melt viscosity*

The formation of block or graft polymers during reactive compatibilization alters both the nature of the interface and the rheological characteristics of the blend. A change in the viscosity ratio (or torque ratio) may also play a role in the shift of the phase inversion composition, since the material with the lower viscosity tends to form the continuous phase [6,7,32,47–53]. The grafting reaction [19,30,49] causes a substantial increase in torque in the Brabender when IA and each of these polyamides are mixed (see Fig. 4).

Which component of a binary blend forms the continuous or dispersed phase can generally be represented as regions on a plot of viscosity (or torque) ratio versus volume fraction (or ratio) of the blend. For non-reactive blends, the viscosity ratio is simply defined by the pure component values at the shear rate of the mixing. However, for reactive systems, the viscosity ratio may be substantially different from this simple ratio, but may be difficult to quantify. Fig. 5 shows an illustrative example where the nylon 6 to SAN25 torque ratio is plotted versus the nylon 6 volume fraction for blends containing 5 wt% IA. For the series of points labeled “uncorrected,” the torque ratio was calculated from the values for pure H-PA (11.5 N m) and SAN25 (6.6 N m) and is the same for all the blends regardless of the blend composition or IA content. The series of points labeled “corrected” take into account the torque changes due to the formation of PA–IA graft polymers using the relationship between IA concentration and the increase in torque shown in Fig. 4.

This correction is based on the assumption that the

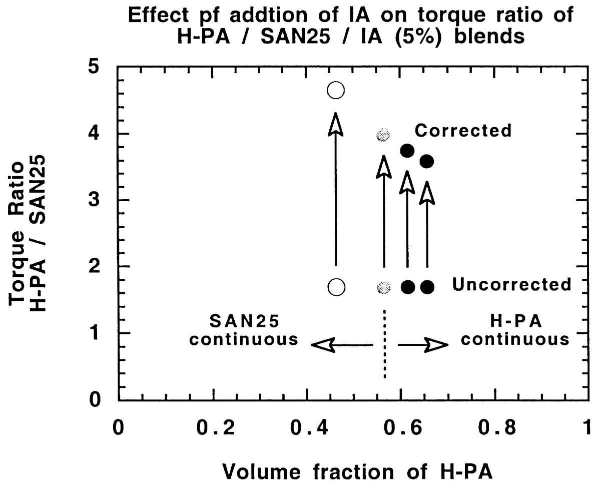

Fig. 5. Effect of addition of IA on torque ratio of H-PA/SAN25/IA blends.

addition of IA has no effect on the torque of the SAN25 phase, but does increase the torque of the nylon 6 phase. The basis for this assumption is that the former is a simple physical process and experiments show a negligible change in torque as IA is added to SAN25; whereas, addition of IA to nylon 6 increases the torque, due to graft formation, as shown in Fig. 4. For these calculations, all of the added IA is assumed to be in the polyamide; that is, for a 47.5/47.5/5 blend the IA content of the polyamide phase is taken as 5/(47.5 + 5) for purpose of reading torque values from Fig. 4. This method gives an upper limit to the viscosity ratio; a more realistic estimate may lie somewhere between the “uncorrected” and “corrected” ratios.

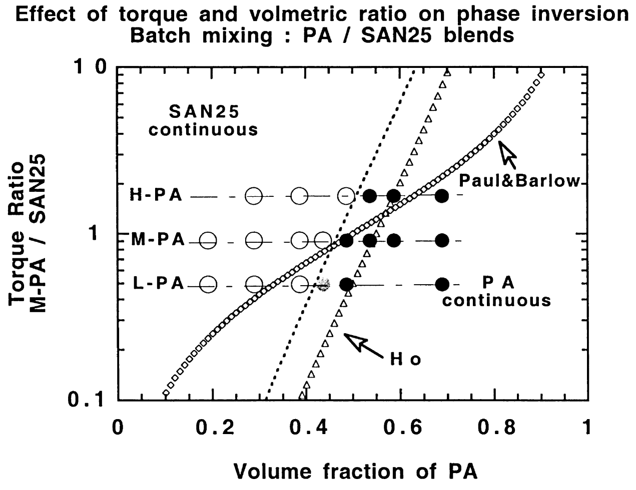

Fig. 6. Relation between torque ratio and polyamide volume fraction on the phase inversion for the uncompatibilized blends prepared in a Brabender batch mixer.

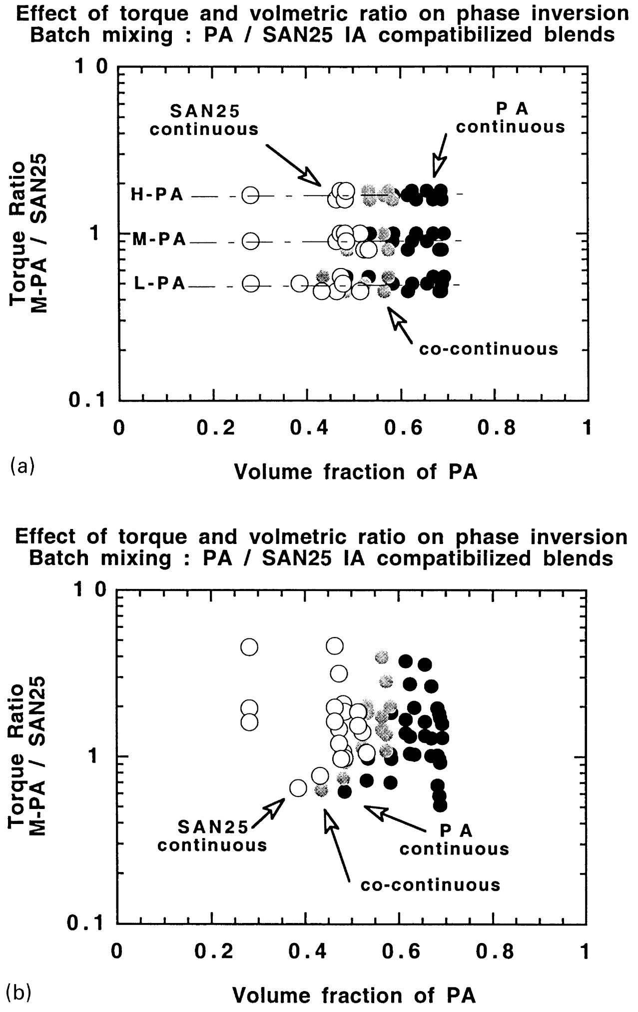

Fig. 7. Relation between torque ratio and polyamide volume fraction on the phase inversion for the IA compatibilized blends prepared in a Brabender batch mixer. The torque increase of nylon 6 phase due to the formation of graft polymer is not taken into account in part (a) but is taken into account in part (b).

3.3. Relationship between composition, torque ratio, and morphology

Fig. 6 maps the phase continuity of nylon 6/SAN25 blends in terms of the nylon 6 volume fraction, ϕ, and the torque ratio of the two pure components. Since there is no reactive compatibilizer present, no correction is necessary and the torque ratio for a given nylon 6 is the same regardless of the composition. A continuous nylon 6 phase is denoted by solid circles, while open circles denote a continuous phase of SAN25; co-continuous phases are denoted by shaded circles. The dotted line represents the region where phase inversion is observed to occur. Two calculated lines, denoted by small, overlapping triangular or square points, will be discussed later.

Fig. 7 shows a similar morphology map for blends containing IA. In Fig. 7a the torque ratio has not been corrected for the grafting reaction that occurs, i.e. the ratio

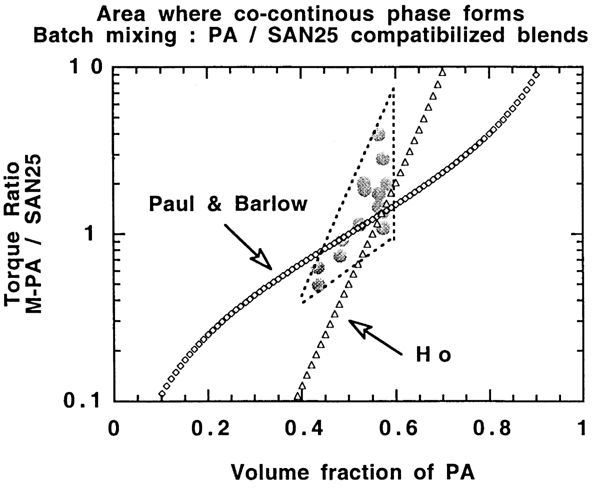

Fig. 8. The composition range where a co-continuous phase forms for the blends compatibilized with IA.

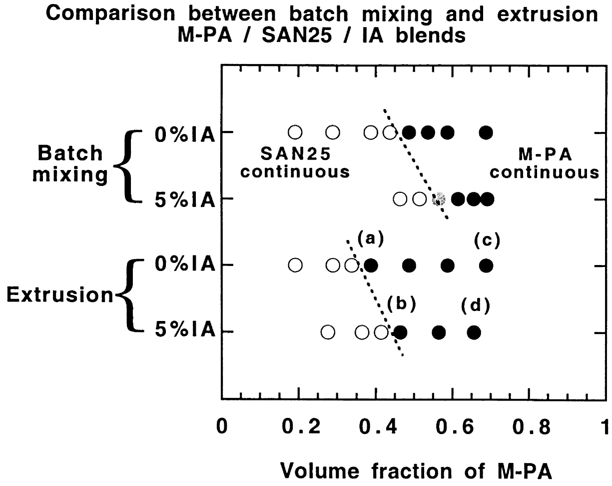

Fig. 9. Comparison between Brabender batch mixing and extrusion on the phase inversion composition for the blends compatibilized with and without IA.

of torque for the pure components is used; whereas, in Fig. 7b the correction for the nylon 6 phase torque caused by reaction described earlier has been applied. In Fig. 7a, some of the data points at the same viscosity ratio have been slightly offset to avoid overlap. Fig. 7b appears to give a more unique delineation of the phase inversion region than does Fig. 7a.

The data points representing a co-continuous phase morphology in Fig. 7b are replotted in Fig. 8. The addition of IA to PA/SAN25 blends not only shifts the phase inversion composition to a higher polyamide volume fraction but also widens the composition region where co-continuous phases form; however, there seems to be a boundary on this area at a nylon 6 volume fraction of around 0.6.

Willemse et al. [54] reported for polystyrene/polyethylene blends that a low interfacial tension results in phase co-continuity over a broad composition range. Miles et al. [55] also suggested that the reduction of the interfacial tension enhances phase co-continuity. On the other hand, Willis et al. [49] reported for polyamide blends with polypropylene or polyethylene that compatibilization using a polyethylene-based ionomer caused narrowing of the region where co-continuous phases formed. Likewise, Dedecker et al. [6] reported that the region of phase co-continuity is much smaller for the compatibilized blends because of the reduced rate of coalescence resulting from compatibilization.

3.4. Prediction of the phase inversion point

Several empirical equations have been proposed for predicting the phase inversion composition in terms of the viscosity ratio [7,32,46,47,53,54,56,57] Paul and Barlow [58] qualitatively suggested such a relation that Jordhamo et al. [59] subsequently cast in the following quantitative form

$$\frac{\eta_1}{\phi_2} = \frac{\eta_1}{\phi_2} \tag{1}$$

where η_i is the viscosity of component i, and ϕ_i is the volume fraction of component i. Miles et al. [60] emphasized that the condition for co-continuity should be expressed by the viscosity ratio at the shear rate prevailing in the mixing device used to prepare the blends. Avgeropoulos et al. [61] introduced the use of the torque ratio. Jordhamo et al. showed that this simple equation describes the experimentally observed phase inversion point for PS/polybutadiene blends. The series of small square points shown in Figs. 6 and 8 were calculated from Eq. (1), using the Brabender torque ratio rather than viscosity.

Ho et al. [62] suggested a modified version of Eq. (1)

$$\frac{\phi_1}{\phi_2} = 1.22\left(\frac{\eta_1}{\eta_2}\right)^{0.29} \tag{2}$$

where the viscosity ratio may be replaced with the torque ratio. This relationship is shown in Figs. 6 and 8 as a series of small triangular points. Neither Eq. (1) nor Eq. (2) fully represents the phase inversion composition of uncompatibilized PA/SAN blends; however, by changing the numerical coefficient in Eq. (2) as shown below

$$\frac{\phi_1}{\phi_2} = 0.887\left(\frac{\eta_1}{\eta_2}\right)^{0.29} \tag{3}$$

a good representation can be obtained. The relationship calculated using Eq. (3) is shown in Fig. 6 as a dotted line.

For compatibilized blends, the rather broad triangular area shown in Fig. 8 defines the region of phase co-continuity, which is not represented by any simple equation. The shift of the phase inversion composition and the widening of the composition range where a co-continuous phase forms

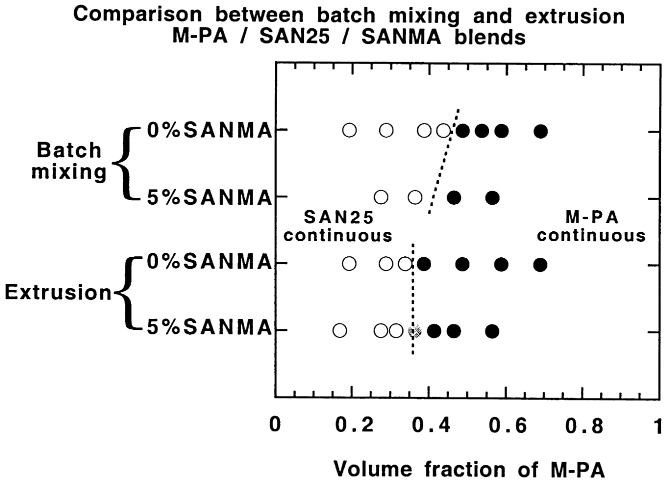

Fig. 10. Comparison between Brabender batch mixing and extrusion on the phase inversion composition for blends with and without SANMA.

complicates the prediction of the phase inversion composition for compatibilized PA/SAN25 blends.

3.5. *Effects of the mixing method and the compatibilizer type*

The type of melt mixing device used can certainly affect the details of blend morphology and may have an influence on the composition where phase inversion occurs. To examine this, the results described above from the Brabender batch mixer are compared here with blends made in a continuous process employing a single screw extruder outfitted with an intensive mixing head. The results are shown in Fig. 9 where the dotted lines represent the phase inversion compositions. The points denoted by the letters (a) to (d) will be discussed later.

In the batch mixer, phase inversion occurs at a M-PA volume fraction of about 0.45 when the blend is not compatibilized but shifts to a M-PA volume fraction of about 0.55 when 5 wt% IA is added. In the extruder, phase inversion occurs at a lower volume fraction of M-PA, viz., around 0.35 for the blends without IA and 0.45 with 5 wt% IA. In both mixers the phase inversion composition shifts to higher nylon 6 volume fractions with addition of IA. The fact that the nylon 6 forms the continuous phase at a lower M-PA volume fraction when mixed in the extruder suggests that either the more intense mixing it provides facilitates the formation of a continuous phase by the more viscous component. Of course, the nature of the compatibilizer may play a role in this behavior so similar experiments were carried out using the SANMA terpolymer as the compatibilizer; the results are shown in Fig. 10. In the batch mixer, the phase inversion composition is shifted from a nylon 6 volume fraction of 0.45 to about 0.40 on addition of 5 wt% SANMA. Thus, in contrast to IA, the addition of SANMA slightly lowers the nylon 6 volume fraction where phase inversion occurs. When mixed in an extruder, phase inversion occurs at a nylon 6 volume fraction of 0.35 with and without SANMA.

Thus, it can be concluded that the phase inversion composition is affected by the mixing method, i.e. the extruder expands the composition range where the nylon 6 forms a continuous phase compared to the batch mixer. The addition of a compatibilizer may or may not affect the phase inversion composition, e.g. addition of IA shifts the phase inversion composition to a higher nylon 6 volume fraction; whereas, the addition of SANMA slightly shifts the phase inversion composition to a lower nylon 6 volume fraction. It is important to understand the reasons for the different responses of these two compatibilizers.

Fig. 11 compares the Brabender torque of binary blends of M-PA with each of these compatibilizers. It is clear that IA results in a significantly larger increase in torque than is the case for SANMA. The chemical and physical differences between these compatibilizers have been discussed by Kudva et al. [42]. They note that for a fixed compatibilizer concentration, the amount of anhydride functionality for SANMA is greater than for IA, while when the amount of methacrylic acid functionality of IA is also taken into account, the possible extent of grafting reaction could be much higher for IA than SANMA. Reaction between the polyamide amine group and the acid functionality is believed to be much slower than with the anhydride. The time available for reaction in the batch mixer is significantly greater than the residence time in the extruder. These chemical issues may have some role in the shift of the phase inversion composition.

3.6. *Morphology stability*

A compatibilizer is typically used for reducing domain size and for stabilizing the morphology of immiscible blends. If an addition of 5 wt% IA fully stabilized the morphology of a nylon 6/SAN25 blend prepared in an extruder, then the morphology of the extrudate should be maintained after an additional mixing step, e.g. in a batch mixer where the shear is less intense than in the extruder. On the

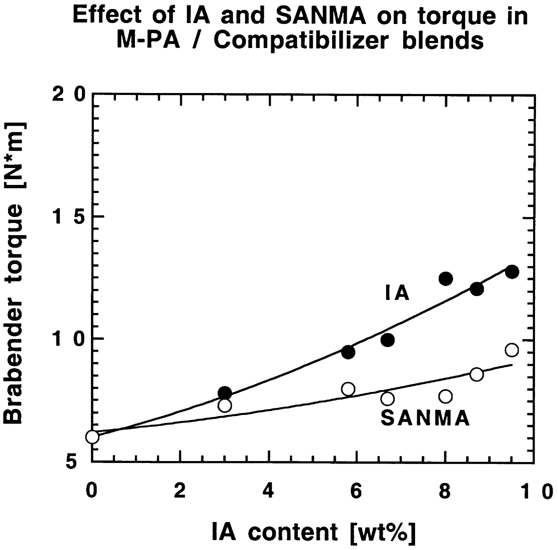

Fig. 11. Effect of the addition of IA or SANMA on torque increase of nylon 6 phase.

other hand, if the morphology is not stable, a blend initially prepared in the extruder and then re-processed in the batch mixer may have a morphology more similar to that of a blend prepared initially in the batch mixer.

It was shown in Figs. 9 and 10 that phase inversion takes place at a lower polyamide volume fraction for the blends prepared in the extruder than in the batch mixer. Extrudates of compositions M-PA/SAN25 = 40/60, point (a) in Fig. 9, and P-MA/SAN/IA = 47.5/47.5/5, point (b) in Fig. 9, each having a nylon 6 continuous phase were given an additional processing history in the batch mixer to determine the morphology stabilization effect by the use of compatibilizers. Sixty grams of the extrudate pellets of these compositions were introduced into a Brabender batch mixer preheated to 240°C, and mixed at 60 rpm for 10 min; this process thoroughly reproduces the same mixing condition of the blends initially prepared in a Brabender batch mixer. After this, the Brabender rotor speed was reduced to 5 rpm, and further mixed for 5 or 10 min. This reduction of the rotor speed alters the balance of drop break-up versus domain coalescence, i.e. the extent of drop break-up is reduced by lowering the shear rate while the rate of domain coalescence is less affected. The validity of this unique Brabender experiment has been verified in the previous reports from our laboratory [45,63].

Figs. 12 and 13 show the evolution of morphology of these two blend compositions as they progress through this processing history. The initial extrudates from the extruder for both blends show a nylon 6 continuous phase (Figs. 12a and 13a). Then these extrudates were mixed in the batch mixer at 60 rpm for 10 min (Figs. 12b and 13b). It is seen in Fig. 12b that complete phase inversion occurs for the uncompatibilized blend; whereas, the transition from nylon 6 continuous phase to SAN25 continuous phase is seen in Fig. 13b for the compatibilized blend. Figs. 12c and 13c show the morphology of these blends after further mixing at a reduced mixing speed (5 rpm) for 10 min in the batch mixer. It is seen in Fig. 12c that domain coalescence occurs at this low speed for the uncompatibilized blend. Fig. 13c

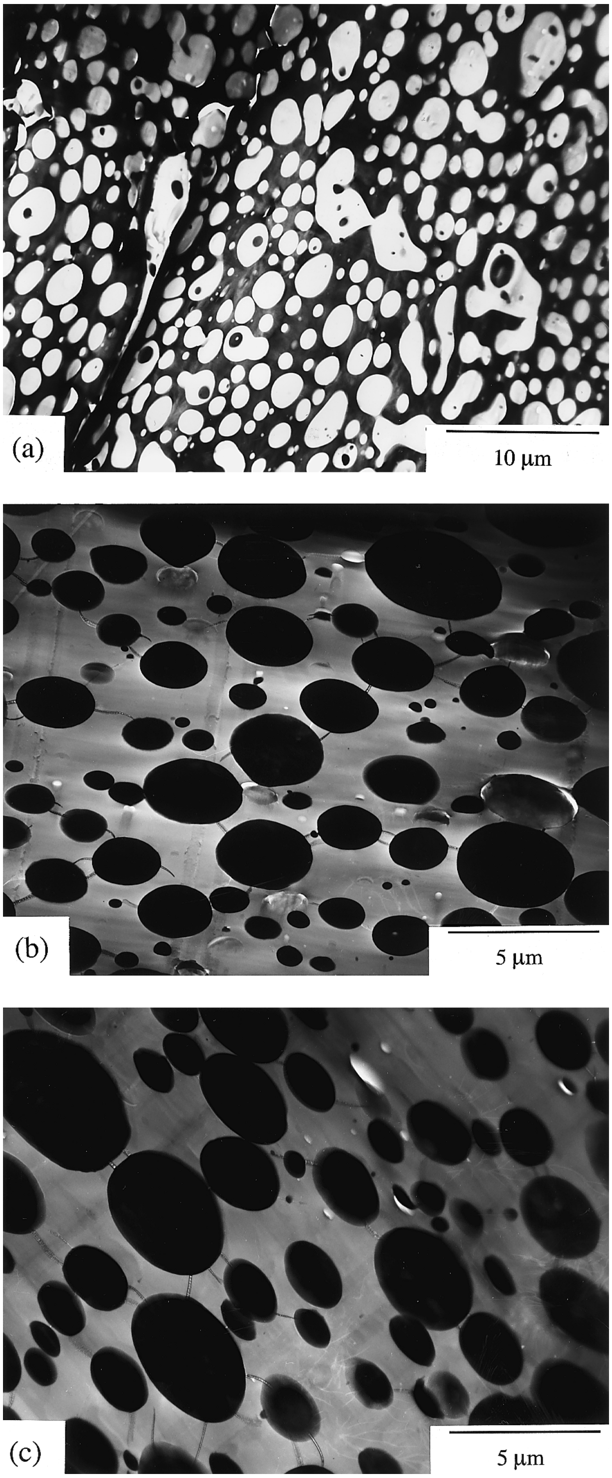

Fig. 12. TEM photomicrographs of M-PA/SAN25 = 40/60 blends: (a) prepared in an extruder; (b) prepared in an extruder, then mixed in a Brabender batch mixer at 60 rpm for 10 min; (c) prepared in an extruder, then mixed in a Brabender batch mixer at 60 rpm for 10 min and additional mixing at 5 rpm for 10 min. The nylon 6 phase has been stained with PTA.

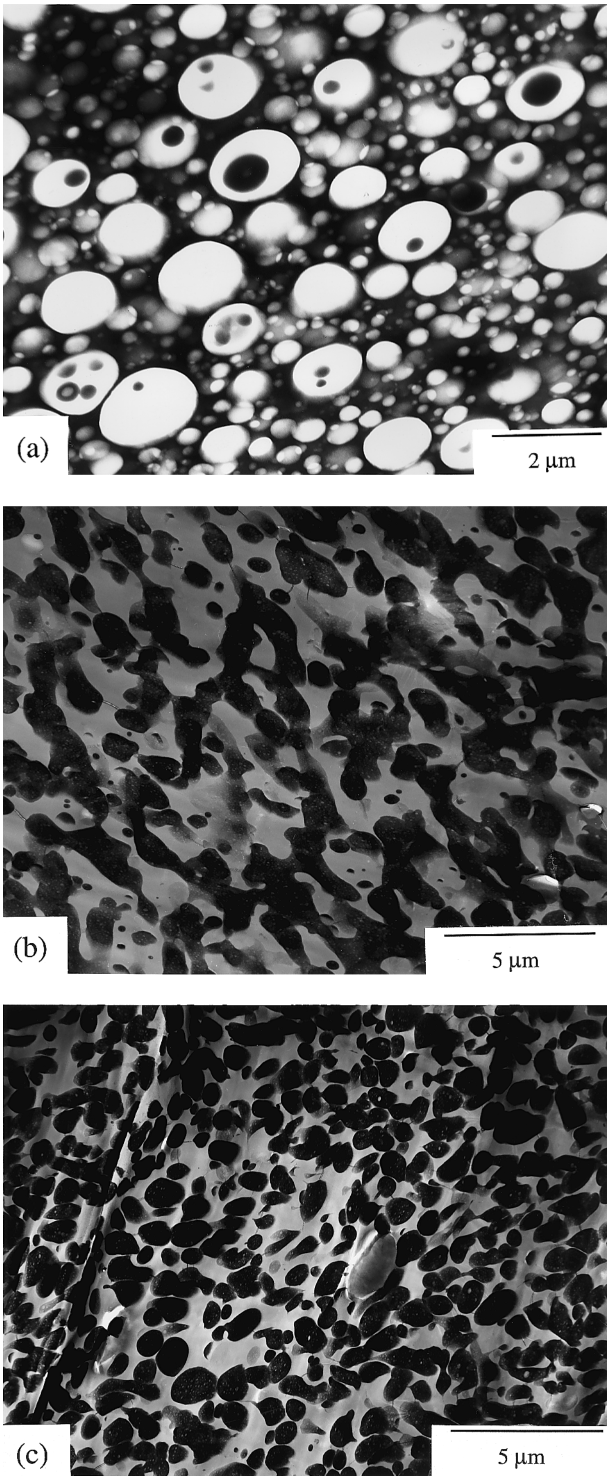

Fig. 13. TEM photomicrographs of M-PA/SAN25/IA = 47.5/47.5/5 blends: (a) prepared in an extruder; (b) prepared in an extruder, then mixed in a Brabender batch mixer at 60 rpm for 10 min; (c) prepared in an extruder, then mixed in a Brabender batch mixer at 60 rpm for 10 min and additional mixing at 5 rpm for 10 min. The nylon 6 phase has been stained with PTA.

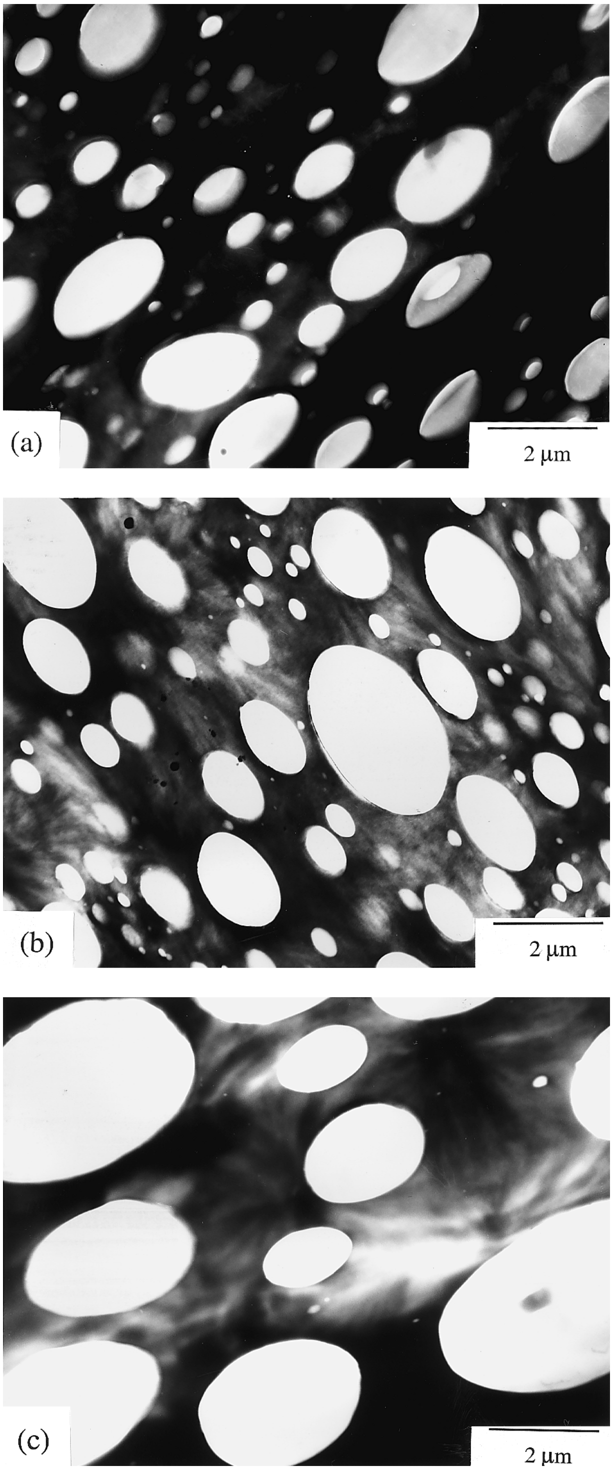

Fig. 14. TEM photomicrographs of M-PA/SAN25 = 70/30 blends: (a) prepared in an extruder; (b) prepared in an extruder, then mixed in a Brabender batch mixer at 60 rpm for 10 min; (c) prepared in an extruder, then mixed in a Brabender batch mixer at 60 rpm for 10 min and additional mixing at 5 rpm for 10 min. The nylon 6 phase has been stained with PTA.

shows the occurrence of complete phase inversion for the compatibilized blend. In addition, it has been found that the blend shown in Fig. 13a shows a co-continuous phase morphology similar to Fig. 13b after the injection molding. This might be caused by the result of less intense shearing during the injection molding process than that experienced in the extruder. Thus, subsequent processing may alter the blend morphology

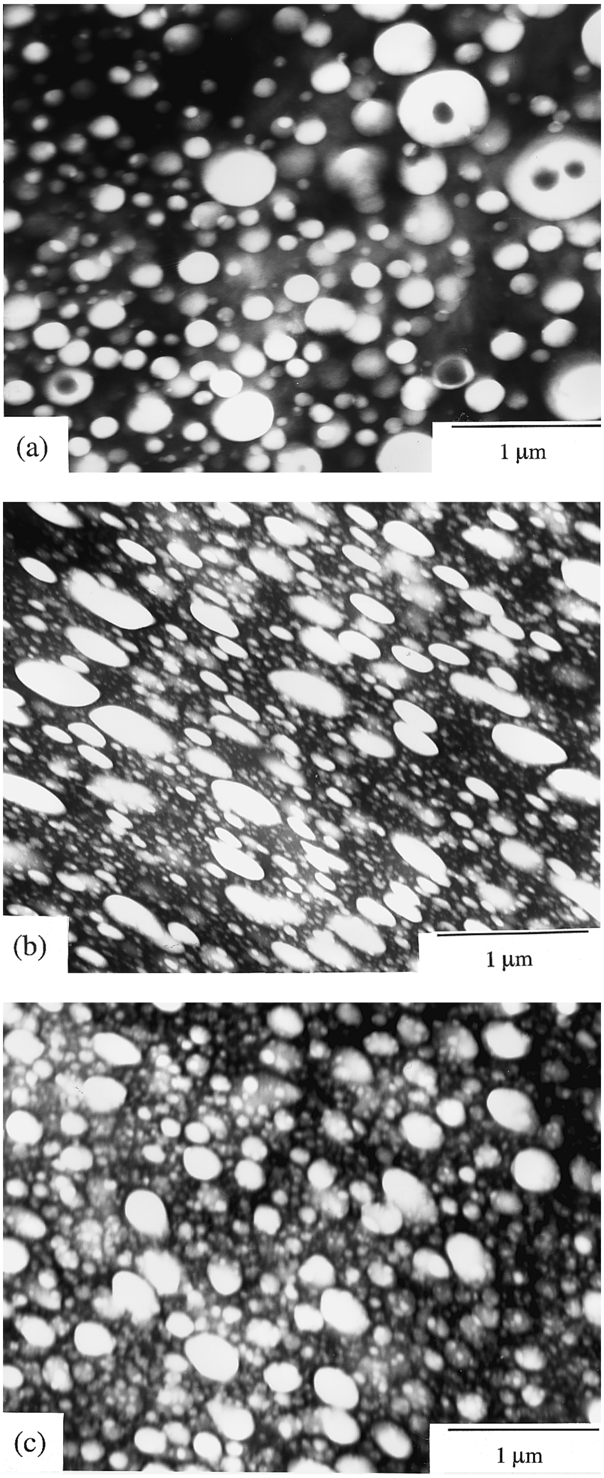

Fig. 15. TEM photomicrographs of M-PA/SAN25/IA = 66.5/28.5/5 blends: (a) prepared in an extruder; (b) prepared in an extruder, then mixed in a Brabender batch mixer at 60 rpm for 10 min; (c) prepared in an extruder, then mixed in a Brabender batch mixer at 60 rpm for 10 min and additional mixing at 5 rpm for 10 min. The nylon 6 phase has been stained with PTA.

regardless of the use of a compatibilizer when the composition is near the phase inversion region.

Figs. 14 and 15 show results for a similar series of experiments at compositions where the blends form a well-defined nylon 6 continuous phase in the batch mixer as well as in the extruder, i.e. M-PA/SAN25 = 70/30, point (c) in Fig. 9, and M-PA/SAN25/IA = 66.5/28.5/5, point (d) in Fig. 9. These compositions are far away the region of phase inversion for these blends. The initial extrudates from the extruder for both blends show a continuous phase of nylon 6 (Figs. 14a and 15a). These extrudates were then mixed in the batch mixer at 60 rpm for 10 min (Figs. 14b and 15b). It is seen that both blends maintain the continuous phase of nylon 6. Figs. 14c and 15c show the morphology of these

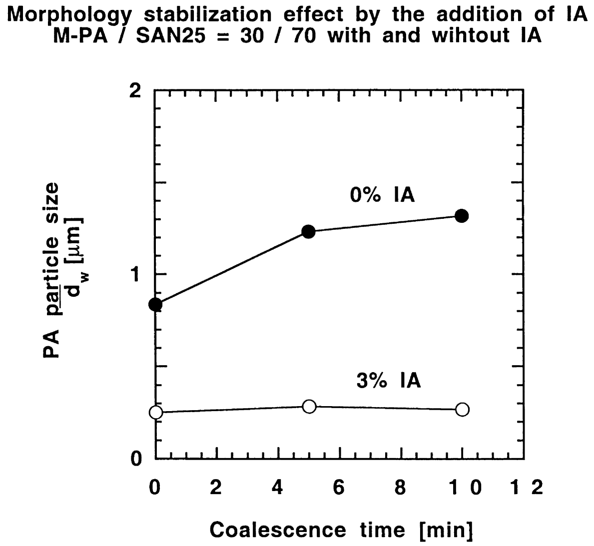

Fig. 16. Average dispersed particle size for M-PA/SAN25 = 30/70 blend uncompatibilized and compatibilized with 3 wt% IA as a function of coalescence time at 5 rpm (time zero corresponds to a blend mixed in a Brabender for 10 min at 60 rpm).

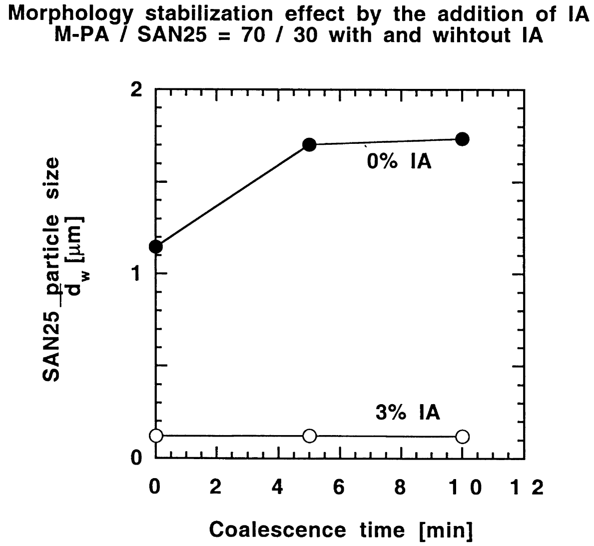

Fig. 17. Average dispersed particle size for M-PA/SAN25 = 70/30 blend uncompatibilized and compatibilized with 3 wt% IA as a function of coalescence time at 5 rpm (time zero corresponds to a blend mixed in a Brabender for 10 min at 60 rpm).

blends after further mixing at a reduced mixing speed (5 rpm) for 10 min. Fig. 14c shows domain coalescence for the uncompatibilized blend during low shear mixing in the batch mixer; whereas, the compatibilized blend maintains the original morphology established in the extruder (Fig. 15b).

Figs. 16 and 17 compare the growth of domain size of compatibilized (3 wt%) and uncompatibilized blends mixed in the Brabender batch mixer. The blend compositions correspond to M-PA/SAN25 = 30/70 in Fig. 16 which forms a stable SAN25 continuous phase, and M-PA/SAN25 = 70/30 in Fig. 17 which forms a stable polyamide continuous phase.

The blends were mixed in the batch mixer at 60 rpm for 10 min and the morphology of these blends were observed. The average domain sizes of these blends are shown in Figs. 16 and 17 at zero coalescence time. Then the blends were mixed further at the reduced speed (5 rpm) for 5 min and 10 min, and the domain sizes were determined. Growth of the domain size occurs after the reduction of the mixing speed for both uncompatibilized blends; whereas, the domain size does not change for the compatibilized blends upon the reduction of the mixing speed.

Thus, the compatibilizers stabilize the blend morphology within the composition range where either component forms a well defined dispersed phase; whereas, the compatibilizers do not stabilize the morphology at compositions near the phase inversion range.

4. Conclusion

The phase morphology and phase inversion behavior of nylon 6/SAN25 compatibilized blends have been studied using an imidized acrylic polymer and a styrene/acrylonitrile/maleic anhydride terpolymer as compatibilizers. The addition of IA causes the phase inversion composition to shift to a higher nylon 6 volume fraction; whereas, the addition of SANMA slightly shifts the phase inversion composition to a lower nylon 6 volume fraction. The use of IA results in a significant increase of the nylon 6 phase viscosity due to the in situ formation of graft polymers during the melt processing; whereas, the addition of SANMA only slightly increases the nylon 6 phase viscosity. The physical and chemical differences between IA and SANMA may play a role in the extent of viscosity increase observed in the two cases. Addition of IA or SANMA does not increase the viscosity of the SAN25 phase. The significant change in the nylon 6 to SAN25 viscosity ratio due to the formation of PA–IA graft polymer may be partially responsible for the shift of the phase inversion composition observed as addition of IA.

The method of the mixing also affects the phase inversion composition. The composition range where the nylon 6 forms a continuous phase extends to a lower nylon 6 volume fraction for blends mixed in the extruder compared to those prepared in the Brabender.

The stabilization of blend morphology by formation of graft copolymers was studied for compositions near the points of phase inversion as well as at compositions away from this region. Accordingly, it has been shown that IA does not stabilize the morphology near the phase inversion composition, but it is very effective for stabilizing the morphology when either of the components forms a well defined dispersed phase.

Acknowledgements

The authors express their appreciation to Mitsubishi Gas Chemical Co. Inc., and Mitsubishi Engineering-Plastics Corp. for their support of various aspects of this research.

References

[1] Utracki LA. Polymer alloys and blends: thermodynamics and rheology. Munich: Hanser, 1989.
[2] Ide F, Hasegawa A. J Appl Polym Sci 1974;18:963.
[3] Angola JC, Fujita Y, Sakai T, Inoue T. J Polym Sci B: Polym Phys 1988;26:807.
[4] Chiang CR, Chang FC. Polymer 1997;38:4807.
[5] Dedecker K, Groeninckx G. Polymer 1998;39:4985.
[6] Dedecker K, Groeninckx G. Polymer 1998;39:4993.
[7] Hietaoja PT, Holsti-Miettinen RM, Seppala J, Ikkala OT. J Appl Polym Sci 1994;54:1613.
[8] Horiuchi S, Matchariyakul N, Yase K, Kitano T, Choi HK, Lee YM. Polymer 1996;37:3065.
[9] Horiuchi S, Matchariyakul N, Yase K, Kitano T. Macromolecules 1997;30:3664.
[10] Horiuchi S, Matchariyakul N, Yase N, Kitano T, Choi HK, Lee YM. Polymer 1997;38:6317.
[11] Lu M, Keskkula H, Paul DR. J Appl Polym Sci 1995;58:1175.
[12] Li H, Chiba T, Higashida N, Yang Y, Inoue T. Polymer 1997;38:3921.
[13] Majumdar B, Keskkula H, Paul DR. Polymer 1994;35:1386.
[14] Majumdar B, Keskkua H, Paul DR. Polymer 1994;35:1399.
[15] Majumdar B, Keskkula H, Paul DR, Harvey NG. Polymer 1994;35:4263.
[16] Majumdar B, Keskkula H, Paul DR. Polymer 1994;35:5453.
[17] Majumdar B, Keskkula H, Paul DR. J Appl Polym Sci 1994;54:339.
[18] Misra A, Sawhnet G, Kumar RA. J Appl Polym Sci 1993;50:1179.
[19] Oshinski AJ, Keskkula H, Paul DR. Polymer 1992;33:268.
[20] Oshinski AJ, Keskkula H, Paul DR. Polymer 1992;33:284.
[21] Oshinski AJ, Keskkula H, Paul DR. Polymer 1996;37:4891.
[22] Oshinski AJ, Keskkula H, Paul DR. Polymer 1996;37:4909.
[23] Oshinski AJ, Keskkula H, Paul DR. Polymer 1996;37:4919.
[24] Padwa AR. J Polym Sci A: Polym Chem 1995;33:2165.
[25] Park I, Barlow JW, Paul DR. J Polym Sci B: Polym Phys 1992;30:1021.
[26] Schaefer R, Kressler J, Neuber R, Muelhaupt R. Macromolecules 1995;28:5037.
[27] Song Z, Baker WF. J Polym Sci A: Polym Chem 1992;30:1589.
[28] Sundararaj U, Macosko CW. Macromolecules 1995;28:2647.
[29] Takeda Y, Keskkula H, Paul DR. Polymer 1992;33:3173.
[30] Triacca VJ, Ziaee S, Barlow JW, Keskkula H, Paul DR. Polymer 1991;32:1401.
[31] Vermeesch I, Groeninckx G. J Appl Polym Sci 1994;53:136.
[32] Zhang X, Yin Z, Yin J. J Appl Polym Sci 1996;62:893.

[33] Lavengood RE, Padwa AR, Harris AF. US Patent 4 713 415, 15 December 1987, Monsanto.

[34] Lavengood RE, Patel R, Padwa AR. US Patent 4 777 211, 11 October 1988, Monsanto.

[35] Lavengood RE, Patel R, Padwa AR. European Patent Application 0220155, 29 April 1987, Monsanto.

[36] Baer M. US Patent 4 584 344, 22 April 1986, Monsanto.

[37] Miyake Y. Japanese Patent 02240158-A, 25 September 1990, Daicel Chem. Ind. K.K.

[38] Aoki Y, Watanabe M. US Patent 4 987 185, 22 January 1991, Monsanto Kasei Co.

[39] Tomono, H., Yamamoto, I., Aoki, Y., U.S. Patent 4 981 906, 1 January 1991, Monsanto Kasei Co.

[40] Majumdar B, Keskkula H, Paul DR. Polymer 1994;35:5468.

[41] Majumdar B, Paul DR, Oshinski AJ. Polymer 1997;38:1787.

[42] Kudva RA, Keskkula H, Paul DR. Polymer 2000;41:239.

[43] Aoki Y, Watanabe M. Polym Engng Sci 1992;32:878.

[44] Mamat A, Vu-Khanh T, Cigana P, Favis BD. J Polym Sci B: Polym Phys 1997;35:2583.

[45] Wildes G, Keskkula H, Paul DR. J Polym Sci B: Polym Phys 1999;37:71.

[46] Bourry D, Favis BD. J Polym Sci B: Polym Phys 1998;36:1889.

[47] Favis BD, Chalifoux JP. Polymer 1988;29:1761.

[48] Favis BD, Therrien D. Polymer 1991;32:1474.

[49] Willis JM, Caldas V, Favis BD. J Mater Sci 1991;26:4742.

[50] Chapleau N, Favis BD. J Mater Sci 1995;30:142.

[51] Favis BD, Willis JM. J Polym Sci B: Polym Phys 1990;28:2259.

[52] Lee CW, Ryu SH, Kim HS. J Appl Polym Sci 1997;64:1595.

[53] He J, Bu W, Zeng J. Polymer 1997;38:6347.

[54] Willemse RC, Posthuma de Boer A, Van Dam J, Gotsis AD. Polymer 1999;40:827.

[55] Miles IS, Zurek A. Polym Engng Sci 1988;28:796.

[56] Willemse RC, Postthuma de Bore A, Van Dam J, Gotsis AD. Polymer 1998;39:5879.

[57] Veenstra H, Van Dam J, Posthuma de Boer A. Polymer 1999;40:1119.

[58] Paul DR, Barlow JW. J Macromol Sci, Rev Macromol Chem C 1980;18:109.

[59] Jordhamo GM, Manson JA, Sperling LH. Polym Engng Sci 1986;26:517.

[60] Miles IS, Zurek A. Polym Engng Sci 1988;28:796.

[61] Avgeropoulos GN, Weissert FC, Biddison PH, Bohm GGA. Rubber Chem Technol 1976;49:93.

[62] Ho RM, Wu CH, Su AC. Polym Engng Sci 1990;30:511.

[63] Hale W, Keskkula H, Paul DR. Polymer 1999;40:365.